Progress In Electromagnetics Research M, Vol. 84, 177–186, 2019

Electrically Small Magnetic Probe with PCA for Near-Field Microwave Breast Tumors Detection

Maged A. Aldhaeebi[1], Thamer S. Almoneef [2], Hussein Attia[3], and Omar M. Ramahi[1, *]

Abstract—In this paper, an electrically small magnetic probe combined with principal components analysis (PCA) technique for microwave breast cancer detection is presented. The proposed magnetic probe is designed as an electrically small square loop antenna integrated with a matching network operating at 528 MHz. The concept of the proposed microwave detection is based on the shift in the resonance frequency of the near-field magnetic probe due to the presence of a tumor. The proposed magnetic probe is highly sensitive in detecting any changes or abnormality in the dielectric properties of the female breast tissues. Detecting the existence of the breast tumors is expected by estimating the variations in the scattering parameters of the probe's response. The PCA is a feature extraction technique applied to accentuate the variance in the sensor responses for both healthy and tumorous cases. It is shown that when a numerical realistic breast phantom with and without tumor cells is placed close to the magnetic probe in the near-field region, the probe is capable of distinguishing between healthy and tumorous tissues. In addition, the probe can identify tumors with various sizes placed in a specific location within the breast. As a proof of concept, the magnetic probe was fabricated and used to detect a 9 mm metallic sphere buried at three different locations inside a lump of chicken meat, mimicking both normal and tumorous breast tissues, respectively. The CST numerical simulations and experimental results demonstrate that the presented technique is an emerging modality for detecting breast tumors through an inexpensive and portable way.

1. INTRODUCTION

Breast cancer is considered as one of the fatal diseases that cause mortality in women worldwide. According to the report by the American Cancer Society in 2019, more than 40,000 women are expected to die of breast cancer [1]. Detecting breast cancer during its early stages of development is a fundamental factor for successful treatment because the tumor size is relatively small and has not spread yet [1]. Currently, computed tomography (CAT) scan, magnetic resonance imaging (MRI) [2, 3], ultrasound, and X-ray mammography are conventional diagnoses techniques used for breast cancer detection [1, 4]. These current modalities have some limitations including ionizing radiation, uncomfortable, low sensitivity, and high cost [4].

To avoid all the shortcomings associated with the current breast cancer detection techniques, researchers have focused their attention on an alternative methodology based on microwaves imaging (MI) which has some advantages for breast cancer detection including inexpensive and non-ionizing modality [4]. MI for breast tumors screening is based on the permittivity and conductivity contrast between normal and tumorous breast tissues at microwave regime [4–6].

Received 13 June 2019, Accepted 10 August 2019, Scheduled 29 August 2019

* Corresponding author: Omar M. Ramahi (oramahi@uwaterloo.ca).

[1] Electrical and Computer Engineering Department, University of Waterloo, Waterloo, Ontario, N2L 3G1, Canada. [2] Electrical Engineering Department, College of Engineering, Prince Sattam Bin Abdulaziz University, Al-Kharj 11942, Saudi Arabia. [3] Electrical Engineering Department, King Fahd University of Petroleum and Minerals (KFUPM), Dhahran, Saudi Arabia.

In the literature, MI is classified into three different techniques for MI breast detection including passive, hybrid, and active methods [7]. Active MI is an emerging technique that may have considerable potential for breast cancer detection. The active MI is classified into two modalities: radar-based and tomography modalities [8]. The tomography approach is usually performed iteratively to reconstruct the dielectric properties of breast tissues by using inverse scattering problem that requires extensive computational resources for producing an image of breast tissues from the recovered microwave data file [8]. A research group at Dartmouth College has developed the first near-field MI system that is based on the tomography modality which has been employed for detecting breast tumors in clinical trials [9]. Caorsi et al. introduced a particle swarm algorithm for 2D microwave imaging for reconstruction of two dimensional dielectric scatterers placed inside an inaccessible domain [10]. Donelli et al. presented microwave imaging technique based on the inversion of time domain data used to detect tumors inserted inside a simple breast model. The developed method was based an evolutionary algorithm for location, detection, and reconstruction of electric properties of breast cancer in a breast phantom [11]. Son et al. developed a preclinical microwave tomography system for breast cancer detection [12]. In this system, a 16-element circular array is placed into an imaging bath having a matching liquid. Each antenna is used for signal transmission and reception over a frequency band from 500 MHz to 3,000 MHz. A matching liquid was used to fill the MI bath to reduce reflections from the breast surface [12].

Radar-based techniques reconstruct the position of the strong reflection signal from the breast tissues by using forward scattering problems where the reflected signals from breast's tissues are analysed to identify the presence of breast tumors [13, 14]. Donelli proposed a microwave system based on a backscattered electromagnetic continuous wave for detecting the respiratory and heart fluctuations of victims trapped under the rubble of collapsed building during an earthquake. The proposed system was based on the backscattered electromagnetic continuous wave which was analyzed using independent component analysis (ICA) algorithm [15]. Several radar-based microwave imaging systems were developed for detecting breast tumors including confocal microwave imaging (CMI), microwave imaging via space time (MIST), and holographic microwave imaging (HMI) [16]. Klemm et al. introduced a prototype of UWB frequency-domain radar-based MI system. The system consists of an aperture array of UWB antennas that are positioned on a section of the hemisphere that conforms to the curved breast shape. The signals are captured by a data acquisition module and transferred to a computer that requires a complex coding algorithm used to process the captured signals [17].

In most of the previously developed microwave imaging systems, the employed sensors are of the conventional antenna types distributed in an array setting with multiple ports to cover or scan the entire breast with microwave signals then collect the signals reflected back from it. Most of the MI systems that employ antennas arrays require complex coding algorithms to process the extensive data obtained from each antenna port or each position of the breast if a mechanically movable single antenna is used [18]. However, such a system is usually sophisticated, bulky, and expensive. As an alternative to antenna arrays, a single antenna has been used with mechanical scanning to obtain readings from multiple points of the breast [19, 20].

In a recent article, a single dipole sensor was used to detect breast tumors of various sizes [19]. The mechanism of tumor detection presented in that work stems from the fact that most human breasts are symmetrical in shape and content. In [19], the probe was placed in close proximity to one of the breasts, and the response of the probe's scattering parameters was recorded. Then, the recorded signal is compared to a reading from the other breast. Due to the symmetrical features of both breasts, a healthy patient should yield an identical reading from both breasts [21]. An indication of the presence of a single or multiple tumors inside the breast is assumed if the reflection coefficient readings are different in either the magnitude or phase. This is because the conductivity and permittivity of breast tumors are higher than normal (healthy) breast tissues [7]. The breast tumors exhibit both high permittivity and permeability compared with surrounding healthy breast tissues. The employed single dipole probe in [19] is considered as an electric probe which is highly sensitive to the changes in the permittivity of the tumors. This is because the interaction of the confined electric field in the dipole gap with permittivity of the tissues is higher than the interaction with the tissues conductivity.

In this work, we propose a magnetic probe for breast tumor detection. The proposed probe is considered as a magnetic-probe which is highly sensitive to any changes in the conductivity of the breast tissues, and the employed magnetic probe exhibits a higher magnetic field than the electric

probe. Because the breast tumors exhibit higher conductivity values, compared with permittivity, than normal breast tissues, the magnetic probes will be highly sensitive than electric probes in terms of detecting the tumors. The mechanism of the proposed detection technique is based on the response of the probe, where the presence of the tumor causes a variation in both the magnitude and phase of the probe response. Because human females almost have two identical breasts, where the left and right breasts are identical in the tissues contents [21, 22], the detection technique introduced here employs two identical probes for testing both breasts at the same time. The reflection coefficients of the two probes are recorded and analyzed using the PCA technique to detect any an abnormality or a tumor in one of the breasts.

In a recent work by Aldhaeebi et al. [19], an electric dipole was employed as a probe to collect the electromagnetic signature with and without a tumor. Since malignant tumors possess a frequency-dependent conductivity that is higher than the surrounding tissues, in this work we propose a *magnetic* probe so that the electromagnetic response is accentuated as compared to an electric dipole. This is attributed to the fact that the magnetic field produced by the magnetic dipole is affected when being placed in close proximity to a conductive material. Such an effect is translated as a shift in the scattering parameter of the magnetic probe as will be shown in the results section.

2. PROBE DESIGN

The magnetic probe employed in this work consists of a square loop with lumped capacitors placed in the middle of each arm as depicted in Fig. 1. The main reason for loading the loop with capacitors is to miniaturize the loop such that it would resonate at lower frequencies. Such a row operating frequency is required to ensure a reasonable penetration level into breast tissues. The loop is hosted on top of a RO4003C Rogers material with a dielectric constant of $\epsilon_r = 3.38$ and thickness of 1.54 mm. Each arm of the loop has a length of $L = 30$ mm and width of $w = 30$ mm. The values of the lumped capacitors are $C_1 = C_2 = 8.2$ pF, $C_3 = 5.7$ pF, $C_4 = 2$ pF, and $C_5 = 160$ nF. Capacitors C_4 and C_5 play a major role in matching the loop with a 50 Ω feeding line at the desired resonance frequency of 528 MHz which lies within the medical band. The loop is then simulated using CST Microwave Studio [23]. The probe simulation response is obtained as shown in Fig. 2(a).

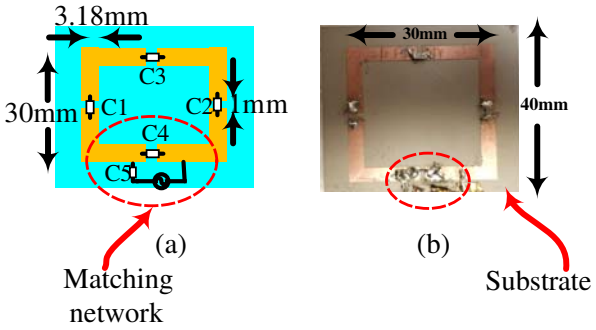

Figure 1. The proposed electrically small probe showing in (a) schematics and (b) fabricated. In both sub-figures, the probe consists of a loop antenna with five capacitors used as matching network.

The fabricated prototype of the proposed probe is shown in Fig. 1(b). The five capacitors are soldered accordingly, and a coaxial cable is placed across the feed of the loop probe. The simulated and measured reflection coefficients of the probe are depicted in Fig. 2(b). It is obvious from the obtained results that the resonance frequencies of both the simulated and measured responses are 528 MHz. However, the measured S_{11} bandwidth is much wider than the simulated one due to the losses of lumped elements which are not accounted for in the simulation.

To investigate the capabilities of the proposed magnetic probe for detecting breast tumor cells, the proposed probe is tested with a realistic female breast through numerical simulations. In this work, we use a 3D anatomically realistic breast phantom model available in CST [24, 25] which are obtained using

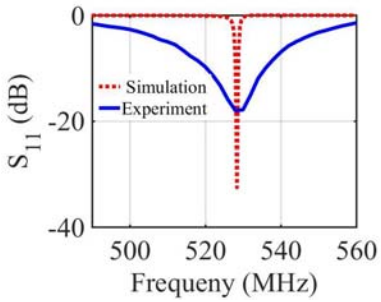

Figure 2. The simulated and measured reflection coefficients of the probe.

the breast MRI datasets from University of Wisconsin online repository [25, 26]. There are four types of breast phantoms defined by the American College of Radiology that are based on the radiographic density of the breast fibrous and glandular tissues that include: (1) almost completely fat, (2) scattered fibroglandular, (3) heterogeneously dense, and (4) Very dense [25]. In this work, the single Cole-Cole model for the frequency-dispersive tissues properties is used to build the heterogeneously dense breast phantom model of ID: 062204 ACR classification: Class No. 3 in CST as [25]:

$$\epsilon(\omega) = \epsilon'(\omega) - j\epsilon''(\omega) = \epsilon_\infty + \frac{\Delta\epsilon}{1 + (j\omega\tau)^{1-\alpha}} + \frac{\sigma_s}{j\omega\epsilon_o} \tag{1}$$

where $\epsilon'(\omega)$ is the frequency-dependant relative permittivity, $\epsilon''(\omega)$ the frequency-dependant dielectric losses, ω the angular frequency, and ϵ_o the free-space permittivity. ϵ_∞, σ_s, τ, and α are parameters of the Cole-Cole model acquired from experimental clinical data.

First, the developed probe is placed at a stand-off distance of 5 mm from the healthy breast phantom as shown in Fig. 3(a). The probe's response is then recorded. Next, a 9 mm tumor is placed at three different locations inside the healthy breast as shown in Fig. 3(b). The dielectric properties of inserted tumor are obtained from tumor surgery as presented in [27]. The three locations namely L1, L2, and L3 are labeled according to the distance between the tumor and the probe where L1 is the closest from the probe, L2 deeper than the first location L1, and L3 the farthest to the probe. The probe response is then recorded for the other breast with the embedded tumor. The probe responses data that contain the magnitude and phase are then analyzed with and without the tumor to determine whether or not the breast is infected with a tumor.

Next, PCA as a feature extraction method [28–30] is employed to emphasize the variation of the probe responses of both normal and tumors cases by extracting important data from the magnitude and phase of the probe's response datasets. These datasets are then represented as orthogonal vectors called principal components [28, 29]. In large datasets, the Principal Component Analysis (PCA) is used to reduce the dimensionality by implementing a vector space transform [28, 29]. The PCA task is to abstract the important information from the dataset and to express this information as a set of new orthogonal variables called principal components [29]. In mathematical terms, eigen-decomposition of

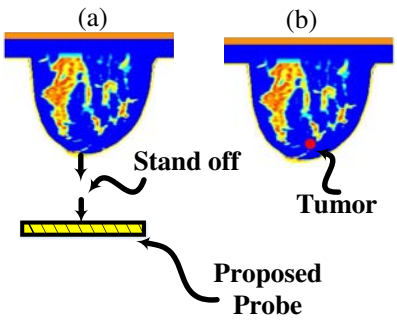

Figure 3. Numerical simulation set-up: (a) Magnetic probe at a stand-off distance of 5 mm away from the 3-D normal breast phantom model. (b) The inserted tumor in the breast model.

positive semi-definite matrices and the singular value decomposition of rectangular matrices are used for finding the principal components [28]. Thus, via mathematical projection, high dimensional original datasets can be reduced to a small number of variables without losing much of the original information to analyze trends, patterns, and outliers [28].

In the proposed microwave detection technique, the reflection coefficient of the proposed magnetic probe which contains the magnitude and phase features is extracted. Here, the feature vectors prior to applying the PCA analysis method are the magnitude and phase of scattering parameters (S_{11}) of the probe. Each discrete value of the reflection coefficient changes with the frequency response. The magnitude and phase of the scattering parameters of the probe are recorded at 201 different frequencies spanning the range 490 to 560 MHz. The first feature dataset, magnitude, is defined by the first and second columns, which contains frequency and magnitude points, respectively. The second feature of datasets, phase, is defined by the first and third columns which includes frequency and phase points, respectively. The data are then entered into the PCA analysis method code to indicate the existence of a tumor inside a breast phantom. Moreover, PCA is used to emphasize or explore the difference between the measured probe responses datasets of the two cases (i.e., with and without tumor). Once the probe scattering parameters of the two examinations of the breast phantom are registered, the probe response is extracted and analyzed with and without PCA as shown in Fig. 4. The results of Fig. 4(a) show the magnitude of S_{11}, and Fig. 4(b) shows the magnitude of S_{11} using PCA. Fig. 4(c) shows the phase of S_{11}, and Fig. 4(d) shows the phase of S_{11} using PCA. It is evident from the results that the difference in magnitude and phase of the reflection coefficient of the probe between the normal and tumorous cases is greater for tumor locations that are closer to the probe.

Then the numerical simulations are extended for detecting three different sizes of tumors placed at a single location. Three different sizes of breast tumors with diameters of 9 mm, 13 mm, and 17 mm are embedded inside the breast phantom to see the capability of the proposed probe for detecting different sizes of the breast tumors as shown in Fig. 3(b). The results are shown in Fig. 5 for the three different tumor sizes. For all tumor sizes, the probe is capable of detecting the presence of tumor tissues. Obviously from the results, larger tumors are easier to detect, where the shift in the frequency response of both magnitude and phase is noticeable compared with a normal case.

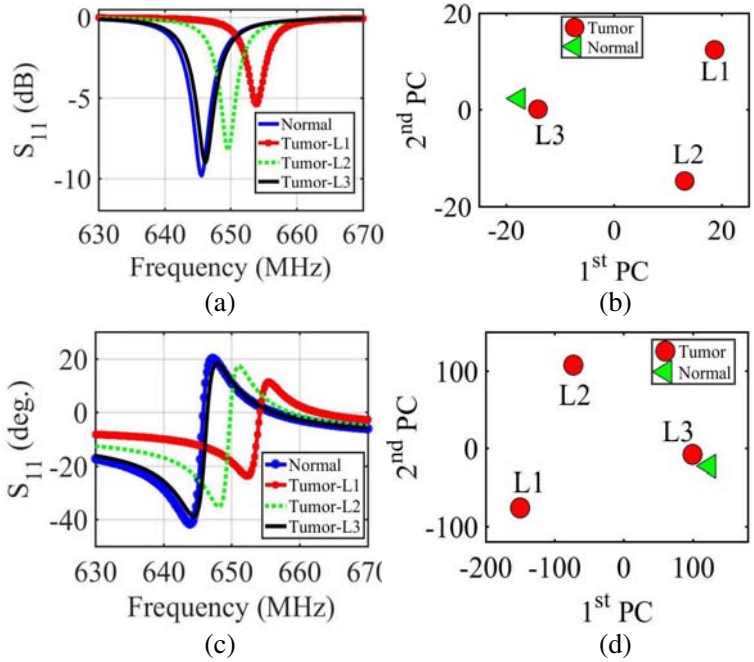

Figure 4. Simulation results of the probe magnitude and phase responses for breast phantom model with and without a 9 mm tumor at three different positions. (a) The S_{11} magnitude, (b) the S_{11} magnitude using PCA, (c) the S_{11} phase and (d) the S_{11} phase using PCA.

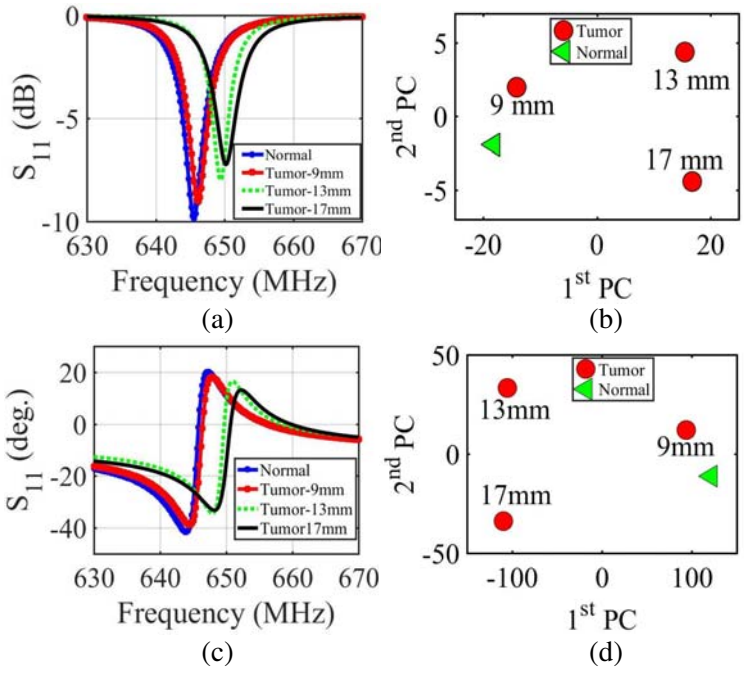

Figure 5. Simulation results of the probe response for detecting three different sizes of breast tumors including: 17 mm, 13 mm and 9 mm inserted at the same location inside the healthy breast phantom. (a) S_{11} magnitude, (b) S_{11} magnitude using PCA, (c) S_{11} phase and (d) S_{11} phase using PCA.

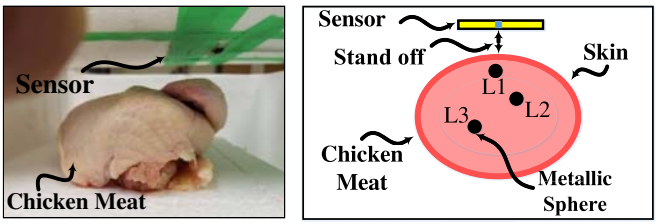

Figure 6. Experiment Procedures: (a) The proposed magnetic probe at a stand-off distance of 5 mm from the chicken meat. (b) A schematic illustrating the experimental setup when inserting a 9 mm metallic sphere at three different positions inside the chicken meat.

3. EXPERIMENTAL VALIDATION

Several experiments are conducted to validate the obtained simulated results. In the experiments, a lump of chicken meat and metallic spheres are used to mimic a breast phantom and a breast tumor, respectively. The chicken meat is placed at a stand-off distance of 5 mm from the fabricated magnetic probe. The whole measurement setup is enclosed in a styrofoam as shown in Fig. 6.

In the experiment, the same test procedure done in the simulation for various tumor locations and sizes is repeated. The obtained results are summarized in Fig. 7 and Fig. 8. Consistent conclusions are obtained from the experiments as compared to the simulations in terms of the sensitivity of the probe to different tumor locations and sizes.

It is noticeable that at location L1, where the 9 mm tumor is closer to the probe, the classification between the healthy and tumorous cases is clear, which indicates higher sensitivity of the detection in both magnitude and phase of the probe's response. Moreover, the classification between the normal breast and breast with tumors is more identifiable in the frequency shift of the S_{11} of the probe.

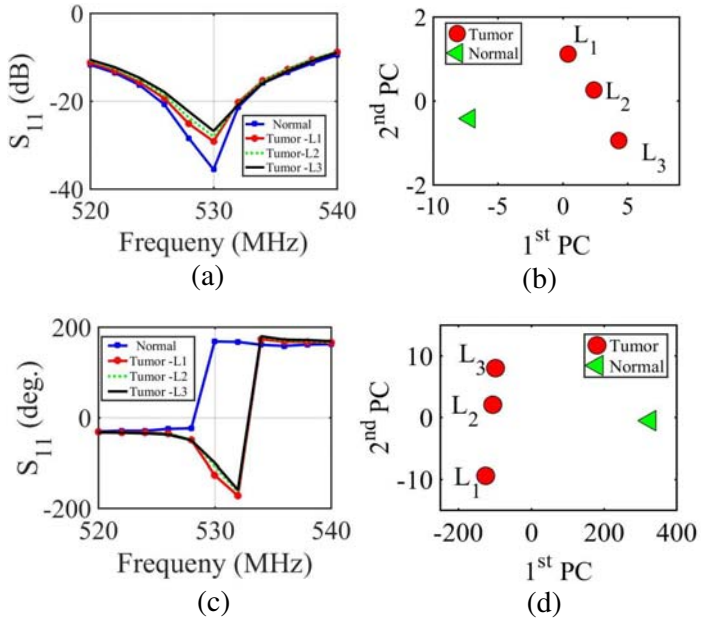

Figure 7. Experiment results showing the probe responses for detecting a 9 mm metallic sphere inserted at three different locations inside the chicken meat. (a) The magnitude of S_{11}, (b) the magnitude of S_{11} using PCA, (c) the phase of S_{11} and (d) the phase of S_{11} using PCA.

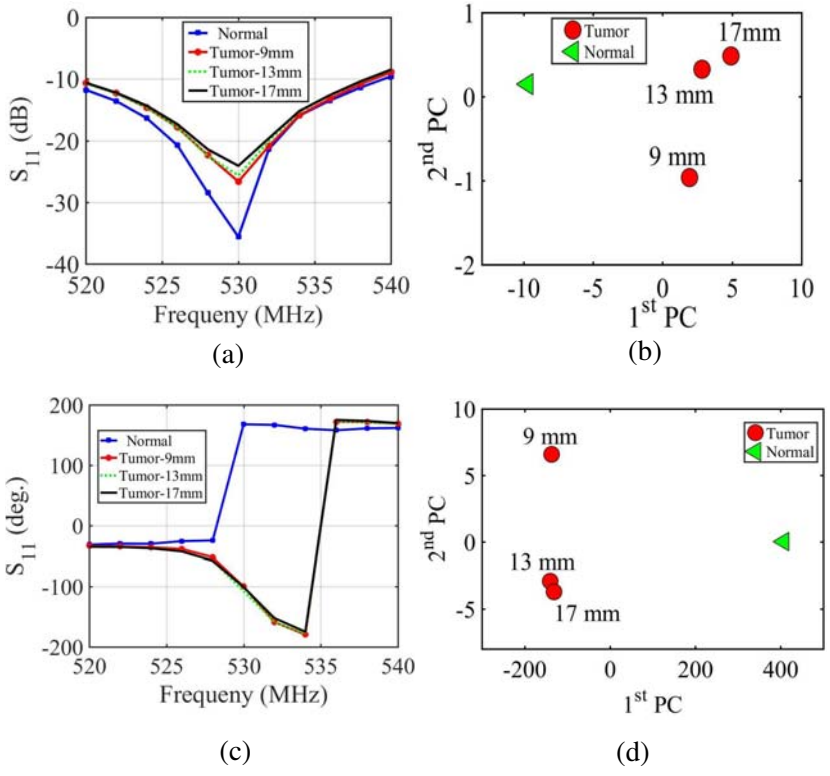

Figure 8. Experimental results showing the probe response for detecting three different sizes of metallic spheres of size 9 mm, 13 mm and 17 mm inserted at the same location inside the chicken meat. (a) S_{11} magnitude, (b) S_{11} magnitude using PCA, (c) S_{11} phase and (d) S_{11} phase using PCA.

For all sizes of the tumor, the probe is capable of detecting the presence of tumor tissues as depicted in Fig. 8. Obviously, from the experimental results, larger tumors are easier to detect. It is evident that as the tumor size increases, the classification using the PCA between the healthy and infected (with different tumor sizes) chicken meats is distinguishable.

4. CONCLUSION

In this work, we introduce a new microwave detection technique for human female breast tumor using an electrically small single loop magnetic probe. The sensing scheme has the advantages of providing non-ionizing, inexpensive, and easy to use method of detection. The detection modality introduced here is used to classify between the healthy and tumorous breasts based on the interaction between the microwave signal of a magnetic-small loop probe and the dielectric properties of the breast tissues of the human female breast. The sensing concept is validated through numerical and experimental tests by detecting tumors placed at different locations and various sizes. The simulation results show the capability of detecting a 9 mm breast tumor embedded in three different locations inside a female realistic breast phantom. The experimental results demonstrate that the proposed probe has higher sensitivity for detecting the presence of a tumor in thee different locations inside a slice of chicken meat having inhomogeneous dielectric variations. The feature extraction method, PCA, is employed to emphasize and enhance the variation in the probe's response to distinguish between normal and tumorous female breasts. We would like to emphasize that the proposed method at this stage can detect tumors in general without indicating the type of tumor whether it is tumorous or benign. Future work will include artificial intelligence methods that will complement the resonator to distinguish between various types of tumors.

ACKNOWLEDGMENT

The authors acknowledge the financial support from King Fahd University of Petroleum and Minerals (KFUPM), Saudia Arabia through DSR project No. SB181027, Hadhramout Establishment for Human Development, Hadhramout, Yemen, Prince Sattam Bin Abdulaziz University, Saudi Arabia, and the Natural Sciences and Engineering Research Council of Canada (NSERC). The authors would like to acknowledge Prof. Susan Hagness group at the University of Wisconsin for providing the numerical breast phantoms.

REFERENCES

1. Society, A. C., "Cancer facts and figures 2019 @ONLINE," [Online]. Available: https://www.cancer.org/content/dam/cancer-org/research/cancer-facts-andstatistics/annual-cancer-facts-and-figures/2019/cancer-facts-and-figures-2019.pdf, 2019.
2. Attaran, A., W. B. Handler, and B. A. Chronik, "2 mm radius loop antenna and linear active balun for near field measurement of magnetic field in MRI-conditional testing of medical devices," *IEEE Transactions on Electromagnetic Compatibility*, 1–8, 2019.
3. Radder, J., M. Woo, P. Van de Moortele, G. Metzger, A. Ertürk, J. Strupp, K. Ugurbil, and G. Adriany, "Optimization and simulation of a 16-channel loop and dipole array for head MRI applications at 10.5 tesla," *2017 International Conference on Electromagnetics in Advanced Applications (ICEAA)*, 1828–1831, Sep. 2017.
4. Wang, L., "Early diagnosis of breast cancer," *Sensors*, Vol. 17, No. 7, 1572, 2017.
5. Obermeier, R. and J. A. Martinez-Lorenzo, "Compressive sensing unmixing algorithm for breast cancer detection," *IET Microwaves, Antennas & Propagation*, Vol. 12, No. 4, 533–541, 2018.
6. Yousefnia, M., A. Ebrahimzadeh, M. Dehmollaian, and A. Madannejad, "A time-reversal imaging system for breast screening: Theory and initial phantom results," *IEEE Transactions on Biomedical Engineering*, Vol. 65, No. 11, 2542–2551, 2018.
7. Conceição, R. C. J. J. Mohr, and M. O'Halloran, *An Introduction to Microwave Imaging for Breast Cancer Detection*, Springer, 2016.

8. Fear, E. C. S. C. Hagness, P. M. Meaney, M. Okoniewski, and M. A. Stuchly, "Enhancing breast tumor detection with near-field imaging," *IEEE Microwave magazine*, Vol. 3, No. 1, 48–56, 2002.
9. Meaney, P. M. M. W. Fanning, D. Li, S. P. Poplack, and K. D. Paulsen, "A clinical prototype for active microwave imaging of the breast," *IEEE Transactions on Microwave Theory and Techniques*, Vol. 48, No. 11, 1841–1853, 2000.
10. Caorsi, S. M. Donelli, A. Lommi, and A. Massa, "Location and imaging of two-dimensional scatterers by using a particle swarm algorithm," *Journal of Electromagnetic Waves and Applications*, Vol. 18, No. 4, 481–494, 2004.
11. Donelli, M., I. J. Craddock, D. Gibbins, and M. Sarafianou, "A three-dimensional time domain microwave imaging method for breast cancer detection based on an evolutionary algorithm," *Progress In Electromagnetics Research*, Vol. 18, 179–195, 2011.
12. Son, S.-H., N. Simonov, H.-J. Kim, J.-M. Lee, and S.-I. Jeon, "Preclinical prototype development of a microwave tomography system for breast cancer detection," *ETRI journal*, Vol. 32, No. 6, 901–910, 2010.
13. Bridges, J. E., "Non-invasive system for breast cancer detection," us Patent 5,704, 355, Jan. 6 1998.
14. Fear, E. C., X. Li, S. C. Hagness, and M. A. Stuchly, "Confocal microwave imaging for breast cancer detection: Localization of tumors in three dimensions," *IEEE Transactions on Biomedical Engineering*, Vol. 49, No. 8, 812–822, 2002.
15. Donelli, M., "A rescue radar system for the detection of victims trapped under rubble based on the independent component analysis algorithm," *Progress In Electromagnetics Research*, Vol. 19, 173–181, 2011.
16. Wang, L., "Microwave sensors for breast cancer detection," *Sensors*, Vol. 18, No. 2, 655, 2018.
17. Klemm, M., I. Craddock, J. Leendertz, A. Preece, and R. Benjamin, "Experimental and clinical results of breast cancer detection using uwb microwave radar," *Antennas and Propagation Society International Symposium, 2008. AP-S 2008. IEEE*, 1–4, 2008.
18. Hassan, A. M. and M. El-Shenawee, "Review of electromagnetic techniques for breast cancer detection," *IEEE Reviews in Biomedical Engineering*, Vol. 4, 103–118, 2011.
19. Aldhaeebi, M. A., T. S. Almoneef, A. Ali, Z. Ren, and O. M. Ramahi, "Near field breast tumor detection using ultra-narrow band probe with machine learning techniques," *Scientific Reports*, Vol. 8, No. 1, 12607, 2018.
20. Bourqui, J., J. M. Sill, and E. C. Fear, "A prototype system for measuring microwave frequency reflections from the breast," *Journal of Biomedical Imaging*, Vol. 2012, 9, 2012.
21. Gazhonova, V., *3D Automated Breast Volume Sonography: A Practical Guide*, Springer, 2016.
22. Chen, J.-H., S. Chan, D.-C. Yeh, P. T. Fwu, M. Lin, and M.-Y. Su, "Response of bilateral breasts to the endogenous hormonal uctuation in a menstrual cycle evaluated using 3d mri," *Magnetic Resonance Imaging*, Vol. 31, No. 4, 538–544, 2013.
23. CST, "Computer simulation technology. cst computer simulation technology ag@ONLINE," [Online]. Available: http://www.CST.com, Sep. 2017.
24. UWCEM, "Breast phantom repository@ONLINE," [Online]. Available: http://uwcem.ece.wisc .edu/ phantomRepository.html, Aug. 2017.
25. Zastrow, E., S. Davis, M. Lazebnik, F. Kelcz, B. van Veem, and S. Hagness, "Database of 3D grid-based numerical breast phantoms for use in computational electromagnetics simulations," [Online]. Available: https://uwcem.ece.wisc.edu/MRIdatabase/InstructionManual.pdf, 2008.
26. Zastrow, E., S. K. Davis, M. Lazebnik, F. Kelcz, B. D. Van Veen, and S. C. Hagness, "Development of anatomically realistic numerical breast phantoms with accurate dielectric properties for modeling microwave interactions with the human breast," *IEEE Transactions on Biomedical Engineering*, Vol. 55, No. 12, 2792–2800, 2008.
27. Lazebnik, M., D. Popovic, L. McCartney, C. B. Watkins, M. J. Lindstrom, J. Harter, S. Sewall, T. Ogilvie, A. Magliocco, T. M. Breslin, et al., "A large-scale study of the ultrawideband microwave dielectric properties of normal, benign and malignant breast tissues obtained from cancer surgeries,"

Physics in Medicine and Biology, Vol. 52, No. 20, 6093, 2007.

28. Richardson, M., "Principal component analysis," URL: http://people.maths.ox.ac.uk/richardsonm/SignalProcPCA. pdf (last access: 3.5. 2013), Aleš Hladnik Dr., Ass. Prof., Chair of Information and Graphic Arts Technology, Faculty of Natural Sciences and Engineering, University of Ljubljana, Slovenia, ales.hladnik@ntf. uni-lj. si, 2009.
29. Abdi, H. and L. J. Williams, "Principal component analysis," *Wiley Interdisciplinary Reviews: Computational Statistics*, Vol. 2, No. 4, 433–459, 2010.
30. Jolliffe, I. T. and J. Cadima, "Principal component analysis: A review and recent developments," *Phil. Trans. R. Soc. A*, Vol. 374, No. 2065, 20150202, 2016.